

# The *Suzaku* X-ray spectrum of NGC 3147

## Further insights on the best “true” Seyfert 2 galaxy candidate

G. Matt<sup>1</sup>, S. Bianchi<sup>1</sup>, M. Guainazzi<sup>2</sup>, X. Barcons<sup>3</sup>, and F. Panessa<sup>4</sup>

<sup>1</sup> Dipartimento di Fisica “Edoardo Amaldi”, Università degli Studi Roma Tre, via della Vasca Navale 84, 00146 Roma, Italy  
e-mail: matt@fis.uniroma3.it

<sup>2</sup> European Space Astronomy Center of ESA, Apartado 50727, 28080 Madrid, Spain

<sup>3</sup> Instituto de Física de Cantabria (CSIC-UC), 39005 Santander, Spain

<sup>4</sup> Istituto di Astrofisica Spaziale e Fisica Cosmica (IASF-INAF), via del Fosso del Cavaliere 100, 00133 Roma, Italy

Received 23 December 2011 / Accepted 12 March 2012

### ABSTRACT

**Context.** NGC 3147 is so far the most convincing case of a “true” Seyfert 2 galaxy, i.e. a source genuinely lacking the broad line regions.

**Aims.** We obtained a *Suzaku* observation with the double aim to study in more detail the iron line complex, and to check the Compton-thick hypothesis for the lack of observed optical broad lines.

**Methods.** The *Suzaku* XIS and HXD/PIN spectra of the source were analysed in detail.

**Results.** The line complex is composed of at least two unresolved lines, one at about 6.45 keV and the other one at about 7 keV, most likely identified with Fe XVII/XIX, the former, and Fe XXVI, the latter. The high-ionization line can originate either in a photoionized matter or in an optically thin thermal plasma. In the latter case, an unusually high temperature is implied. In the photoionized model case, the large equivalent width can be explained either by an extreme iron overabundance or by assuming that the source is Compton-thick. In the Compton-thick hypothesis, however, the emission above 2 keV is mostly due to a highly ionized reflector, contrary to what is usually found in Compton-thick Seyfert 2s, where reflection from low ionized matter dominates. Moreover, the source flux varied between the *XMM-Newton* and the *Suzaku* observations, taken 3.5 years apart, confirming previous findings and indicating that the size of the emitting region must be smaller than a parsec. The hard X-ray spectrum is also inconclusive on the Compton-thick hypothesis. Weighting the various arguments, a “true” Seyfert 2 nature of NGC 3147 seems to be still the most likely explanation, even if the “highly ionized reflector” Compton-thick hypothesis cannot at present be formally rejected.

**Key words.** galaxies: active – X-rays: galaxies – galaxies: Seyfert – galaxies: individual: NGC 3147

## 1. Introduction

NGC 3147 ( $z = 0.009346$ ) is at present the most convincing example of a “true” Seyfert 2 galaxy (Bianchi et al. 2008; Shi et al. 2010; Tran et al. 2011). In such sources the lack of detection of broad emission lines in the optical/UV spectra cannot be explained by the obscuration of the broad line regions (BLR) – as it is the case for “normal” Seyfert 2s in the so far very successful Unification models (Antonucci 1993) – but requires their absence.

In fact, *simultaneous* X-ray and optical spectroscopy have demonstrated that in this source the BLR is lacking at the same time when the nucleus is seen unobscured (Bianchi et al. 2008). The X-ray *XMM-Newton* observation, albeit rather short (less than 20 ks), was good enough to put a tight constraint on the column density of any obscuring material along the line-of-sight. The same observation also indicated complex iron line emission, but the short exposure time did not permit a detailed analysis.

It has been suggested (Nicastro 2000; Nicastro et al. 2003; Elitzur & Shlosman 2006) that at low accretion rates (and thence low luminosities) the BLR cannot form. Indeed, NGC 3147 is a low (even if not extremely so) luminosity source accreting at a low rate (bolometric luminosity  $L \sim 5 \times 10^{42}$  erg s<sup>-1</sup>,  $L/L_{\text{Edd}} \sim 10^{-4}$ , Bianchi et al. 2008).

A possible alternative explanation for the peculiar characteristics of NGC 3147 is that the source is Compton-thick. In fact, the simultaneous lack of BLR and absorption can be explained if

the absorber is so thick to completely obscure the nuclear emission below 10 keV. In this case, the observed emission should be due to reflection off circumnuclear matter, but X-rays could pierce through the absorbers above 10 keV. The hard X-ray coverage offered by *Suzaku* is the best tool at present to test it.

With the dual goal of studying in more detail the iron line emission and to check the Compton-thick explanation for this source, we asked for, and obtained, a long (150 ks) *Suzaku* observation.

The paper is organized as follows. The observation and data reduction are described in Sect. 2, while the data analysis is presented in Sect. 3. Results are discussed and summarized in Sect. 4.

## 2. Observation and data reduction

NGC 3147 was observed by *Suzaku* on 2010, May 24, for 150 ks (OBSID 705054010). X-ray Imaging Spectrometer (XIS) and Hard X-ray Detector (HXD) event files were reprocessed with the latest calibration files available (2011-06-30 release), using `FROOTS` 6.11 and *Suzaku* software Version 18, adopting standard filtering procedures. Source and background spectra for all the three XIS detectors were extracted from circular regions with radius of 167 pixels ( $\approx 175$  arcsec), avoiding the calibration sources. Response matrices and ancillary response files were generated using `XISRMFGEN` and `XISSIMARFGEN`. We downloaded the “tuned”

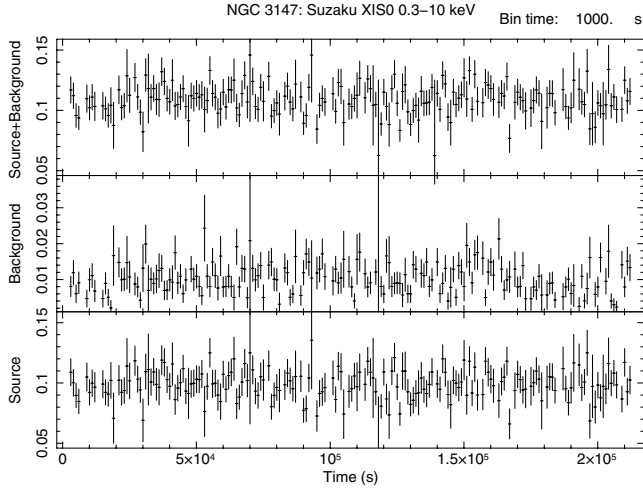


**Fig. 1.** XIS0 light curve. *Upper panel:* count rates in the source extraction region. *Medium panel:* count rates in the background. *Lower panel:* background-subtracted source count rates.

non-X-ray background (NXB) files for our HXD/PIN data provided by the HXD team<sup>1</sup> and extracted source and background spectra using the same good time intervals. The PIN spectrum was then corrected for dead time, and the exposure time of the background spectrum was increased by a factor of 10, as required. Finally, the contribution from the cosmic X-ray background (CXB) was subtracted from the source spectrum, simulating it as suggested by the HXD team.

The XIS spectra were fitted between 0.5 and 10 keV. The normalizations of XIS1 and XIS3 with respect to XIS0 were left free in the fits, and always resulted in agreement to within 3%. A constant factor of 1.16 was used instead between the PIN and the XIS0, as recommended for observations taken in the XIS nominal position. In the following, all the PIN fluxes are given with respect to the XIS0 flux scale, which is 1.16 times lower than the HXD absolute flux scale.

In the following, quoted statistical errors correspond to the 90% confidence level for one interesting parameter ( $\Delta\chi^2 = 2.71$ ), unless otherwise stated. The adopted cosmological parameters are  $H_0 = 70 \text{ km s}^{-1} \text{ Mpc}^{-1}$ ,  $\Omega_\Lambda = 0.73$ , and  $\Omega_m = 0.27$  (i.e., the default ones in xspec 12.7.0: Arnaud 1996). We use the Anders & Grevesse (1989) chemical abundances and the photoelectric absorption cross-sections by Balucinska-Church & McCammon (1992).

### 3. Data analysis and results

The light curve is shown in Fig. 1. No significant variability is detected. For the spectral analysis, therefore, we used spectra integrated over the whole observation.

#### 3.1. The XIS spectra

We first analyzed the XIS spectra. A simple power law model (plus Galactic absorption,  $N_{\text{H,G}} = 3.64 \times 10^{20} \text{ cm}^{-2}$ , Dickey & Lockman 1990) gives a poor fit ( $\chi^2/\text{d.o.f.} = 604.1/482$ ). The most prominent features in the residuals are apparent at the energies of the iron line complex (see Fig. 2). We therefore added two narrow emission lines, with energies free to vary around 6.4

<sup>1</sup> See [ftp://legacy.gsfc.nasa.gov/suzaku/data/background/pinnxb\\_ver2.0\\_tuned/](ftp://legacy.gsfc.nasa.gov/suzaku/data/background/pinnxb_ver2.0_tuned/)

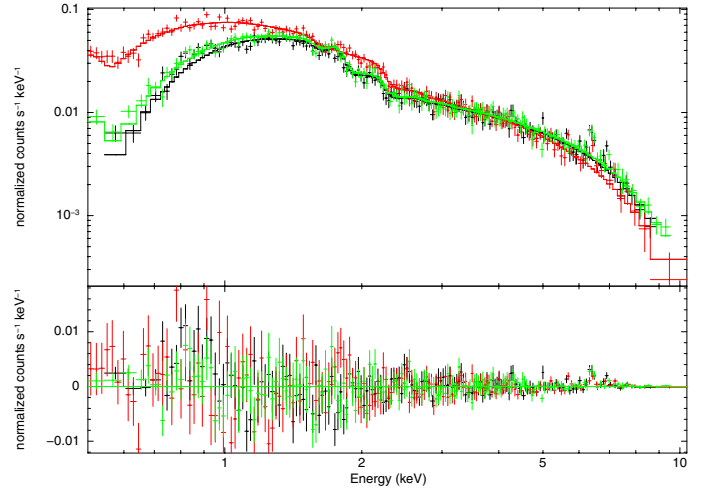


**Fig. 2.** Best fit model and residuals fitting the XIS spectra with a simple power law plus Galactic absorption.

and 7 keV (see next section), which improves significantly the quality of the fit ( $\chi^2/\text{d.o.f.} = 496.4/478$ ). The power law index is  $1.745 \pm 0.014$ . The inclusion of either a warm absorber or a Compton reflection component is not required by the data ( $\Delta\chi^2 = -2.4$  and  $-2.8$ , respectively), while addition of a second power law improves the fit quality ( $\chi^2/\text{d.o.f.} = 481.3/476$ ; the improvement is significant at the 99.94% confidence level, according to the F-test). The power law indices are  $3.50^{(+0.42)}_{(-0.69)}$  and  $1.689^{(+0.022)}_{(-0.018)}$ . The 0.5–2 (2–10) keV flux is  $8.39 \times 10^{-13}$  ( $1.64 \times 10^{-12}$ )  $\text{erg cm}^{-2} \text{ s}^{-1}$ , corresponding to a (absorption corrected) luminosity of  $1.8 \times 10^{41}$  ( $3.2 \times 10^{41}$ )  $\text{erg s}^{-1}$ .

Finally, no intrinsic absorption is detected. The upper limit to the column density of any neutral absorber at the redshift of the source is  $5 \times 10^{20} \text{ cm}^{-2}$ .

#### 3.1.1. Comparison with the XMM-Newton results

We then compared the *Suzaku* spectrum with the *XMM-Newton* one (Bianchi et al. 2008). *XMM-Newton* observed NGC 3147 on 2006, October 6 (i.e. about three and half year earlier), with a net exposure time of 14 ks in the EPIC-pn instrument. We re-extracted the spectrum with the same procedure described in Bianchi et al. (2008), but using the latest version of SAS (11.0.1) and of the calibration files.

According to Bianchi et al. (2008), we fitted the spectrum with a power law absorbed by both Galactic and intrinsic matter, and two narrow gaussian lines. The fit is good ( $\chi^2/\text{d.o.f.} = 93.6/106$ ). The power law index is  $1.62 \pm 0.05$ , the column density of the local absorber is  $< 3.2 \times 10^{20} \text{ cm}^{-2}$ , the energies of the two lines are  $6.471^{(+0.089)}_{(-0.065)}$  keV and  $6.798^{(+0.083)}_{(-0.072)}$  keV and their fluxes are  $2.8(\pm 1.6) \times 10^{-6} \text{ ph cm}^{-2} \text{ s}^{-1}$  (*EW* of 189 eV) and  $2.4(\pm 1.5) \times 10^{-6} \text{ ph cm}^{-2} \text{ s}^{-1}$  (*EW* of 172 eV), respectively. All these values are consistent within the errors with those of Bianchi et al. (2008). The 0.5–2 (2–10) keV flux is  $5.78 \times 10^{-13}$  ( $1.43 \times 10^{-12}$ )  $\text{erg cm}^{-2} \text{ s}^{-1}$ .

Comparing the *XMM-Newton* and *Suzaku* results, a variation, most prominent in the soft band, is found. This is shown in Fig. 3, where the *XMM-Newton* best fit model is superposed to the *Suzaku*/XIS1 spectrum. The variation can be explained either as a steepening of the power law component or, better, with different variations of the soft and hard X-ray component, the

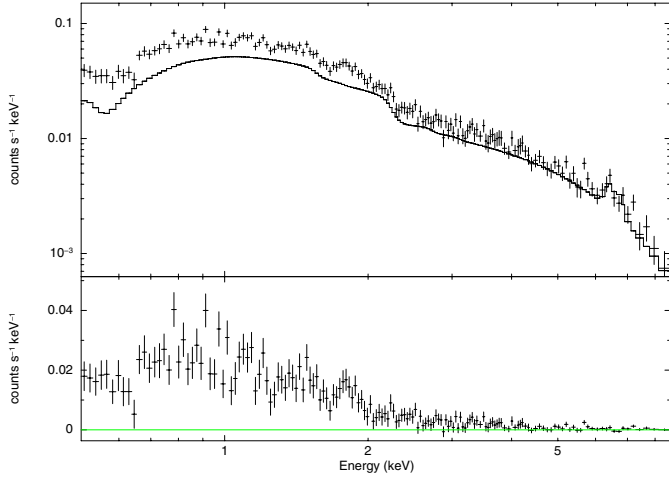


**Fig. 3.** The *Suzaku*/XIS1 spectrum and residuals when the best fit model for the *XMM-Newton* observation is superimposed.

former varying most. An explanation purely in terms of a variation of the local absorber is, instead, not viable.

This result confirms that the source is variable on time scales of years. In fact, the measured 2–10 keV flux, in units of  $10^{-12}$  erg cm $^{-2}$  s $^{-1}$ , has been measured as 1.6 in September 1993 (with *ASCA*: Ptak et al. 1996), 2.3 in November 1997 (with *BeppoSAX*: Dadina 2007) and 3.7 in September 2001 (with *Chandra*: Terashima & Wilson 2003). That the variation cannot be due to a confusing source is demonstrated by the fact that the highest flux has been measured by the best spatial resolution satellite.

### 3.2. The iron line complex

We then studied in more detail the iron line complex. While the iron line properties in the *XMM-Newton* and *Suzaku* observations are roughly consistent, the much better statistics in the *Suzaku* observation due to the longer exposure time allows for a more detailed analysis. To this end, we limited for simplicity the analysis to the XIS instruments, and the energy range to the 4–10 keV band. In Fig. 4, the data and best fit model are shown, after removal of any emission line from the fit. The presence of two emission lines is clear, one around 6.4 keV, to be attributed to  $K\alpha$  emission from neutral or low ionization iron, the other around 7 keV, likely due to either (or both) hydrogen-like (i.e. Fe XXVI) iron emission or  $K\beta$  emission from low ionization iron. We therefore fitted the spectrum with a model composed by a single power law plus three narrow ( $\sigma = 0$ ) emission lines, with rest-frame energies fixed at 6.4 keV (neutral iron,  $K\alpha$ ), 6.96 keV (hydrogen-like iron,  $K\alpha$ ), and 7.06 keV (neutral iron,  $K\beta$ ). The fit is good ( $\chi^2/\text{d.o.f.} = 116.2/120$ ), but some wiggles are apparent in the residuals around the  $K\alpha$  neutral iron line. Letting the energy of that line free to vary, a significantly better fit is found ( $\chi^2/\text{d.o.f.} = 99.5/119$ ), with a line energy of about 6.45 keV. No improvement, instead, is found letting the width of that line free to vary ( $\sigma < 63$  eV), nor including the He-like iron line (upper limit to the flux of  $5.5 \times 10^{-7}$  ph cm $^{-2}$  s $^{-1}$ , corresponding to an equivalent width of 35 eV). Not surprisingly, given the narrowness of the line, no improvement is found with a relativistic profile (*DISKLINE* model), and the inner disk radius is very large (hundreds of gravitational radii). Even in the relativistic line model, an intrinsic line energy at 6.45 keV is strongly preferred by the fit.

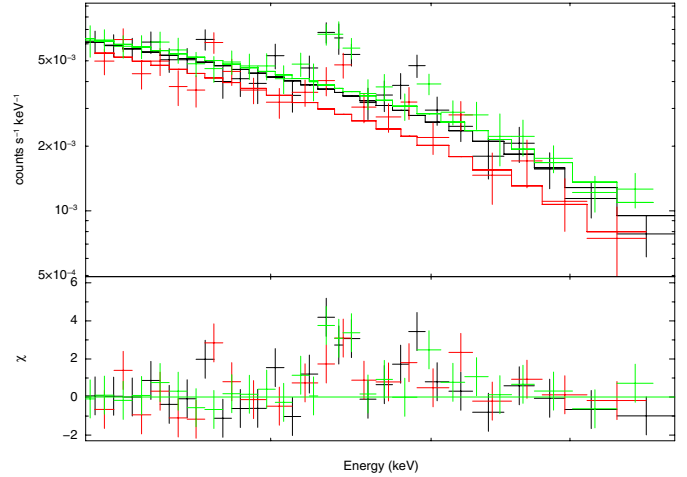


**Fig. 4.** Data and best fit model between 5 and 9 keV. The model is the best fit one (see text), but without any emission lines. Line emission around 6.4 keV and 7 keV is apparent.

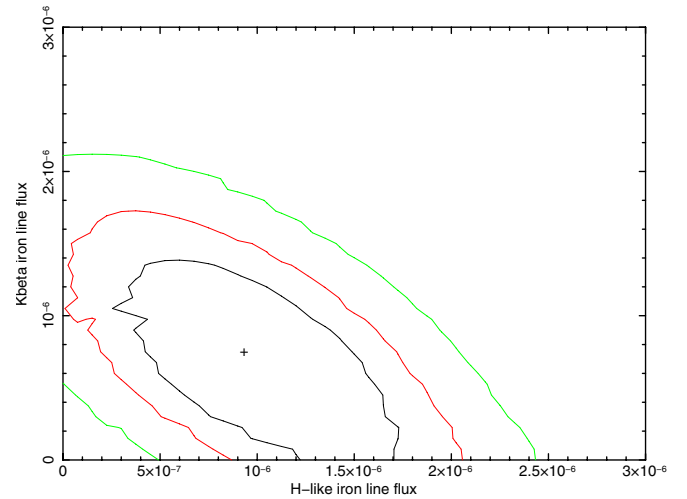


**Fig. 5.** Contour plot of the  $K\beta$  low-ionization line flux vs. the hydrogen-like  $K\alpha$  line flux.

The results are summarized in Table 1. The line fluxes are consistent within the errors to those derived from the *XMM-Newton* spectra. While the hydrogen-like line is only marginally detected and the  $K\beta$  line is formally an upper limit, this of course does not mean that there is no significant line emission at that energy, but simply that the quality of the data is not good enough to accurately determine the parameters of the lines simultaneously. This is best seen in Fig. 5, where the contour plot of the fluxes of the two lines is shown: a simultaneous lack of emission for the two lines is in fact not allowed.

#### 3.2.1. The low ionization iron line

The rest-frame energy of the low ionization  $K\alpha$  iron line is significantly larger than (and not consistent with) 6.4 keV, the energy for neutral iron. We are not aware of any major problem in the energy calibration of the XIS detectors and indeed, fitting the Mn  $K\alpha$  doublet and the  $K\beta$  in the calibration spectra, we found energies consistent with the intrinsic ones. Letting the energy of the line free to vary independently in the three XISs, similar values are found. We therefore conclude that the iron is truly ionized.

**Table 1.** Best-fit parameters for the iron lines.

	$E$ (keV)	Flux ( $10^{-6}$ ph cm $^{-2}$ s $^{-1}$ )	$EW$ (eV)
Low ionized $K\alpha$	$6.452^{+0.021}_{-0.015}$	$3.27 \pm 0.61$	$195 \pm 36$
H-like	6.96	$0.93 \pm 0.89$	$63 \pm 60$
Low ionized $K\beta$	7.06	<1.61	<111

According to House (1967), the best-fit energy corresponds to Fe XVII/XIX, where iron emission should be suppressed by resonant trapping (Ross & Fabian 1993; Matt et al. 1993, 1996). To avoid this effect, the matter should be very optically thin, which is ruled out by the large  $EW$  (almost 200 eV), or very turbulent, so reducing the effective optical depth at the line core. Recent and more refined calculations by Garcia et al. (2011), however, show that suppression is not so efficient and that significant emission from the abovementioned ions is possible. In this case, we do not expect any  $K\beta$  line emission, because for those ions the M shell is no longer populated, and therefore the line emission at about 7 keV should be entirely due to the hydrogen-like iron line.

### 3.2.2. The high ionization iron line

Setting the  $K\beta$  line to zero, the H-like line flux is  $1.44(\pm 0.59) \times 10^{-6}$  ph cm $^{-2}$  s $^{-1}$  (see also Fig. 5), with an equivalent width of about 100 eV $^2$ , and  $\chi^2/\text{d.o.f.} = 101.5/120$ . An upper limit of 35:100 to the ratio between helium- and hydrogen-like lines (as derived from the respective fluxes) implies high values of the ionization parameter, such that the  $EW$  of the hydrogen line should be, for a solar iron abundance, only a few eV with respect to the total continuum (Bianchi & Matt 2002). The required factor of (at least) 10–20 iron overabundance is rather extreme, even if not fully inconsistent with the  $EW$  of the low ionization line (which is a factor 2–3 larger than expected for solar abundance, in agreement with the calculations of Matt et al. 1997, for optically thick matter with a similar iron overabundance).

On the other hand, such large equivalent widths could be explained if the source is Compton-thick and the observed emission comes from reflection in two physically distinct mirrors, one at low and the other at high ionization, with no direct emission. To test this hypothesis, we fitted the spectrum with a power law (representing reflection from highly ionized matter), a Compton reflection component (to account for reflection from low ionized matter), plus two Gaussian lines, one free to vary around 6.4 keV and the other fixed to 6.96 keV. The value of  $R$ , the relative amount of Compton reflection with respect to the power law component, was fixed to 2, which is the value corresponding to the observed  $EW$  of the 6.4 keV line. This translates to a 2–10 keV flux from the high ionization reflector 7 times larger than the low ionization component, a quite unusual configuration in Compton-thick sources where it is the low ionization reflection which generally dominates. The fit is good ( $\chi^2/\text{d.o.f.} = 107.8/120$ ), even if slightly worse than with a simple power law. The H-like line flux is now  $0.97^{(+0.77)}_{(-0.60)} \times 10^{-6}$  ph cm $^{-2}$  s $^{-1}$ , corresponding to an  $EW$  with respect to the high ionized reflection only of about 80 eV, a value consistent with what is expected from the large ionization parameter values implied by the absence of the He-like line (Bianchi & Matt 2002).

<sup>2</sup> Again, assuming a relativistic profile a fit as good as the one with a Gaussian line is obtained, but with a very large inner radius.

Alternatively, this line may be emitted in a high temperature, optically thin thermal plasma. A 0.5–10 keV fit with the MEKAL model (iron abundance fixed to solar) instead of the 7 keV Gaussian line is acceptable ( $\chi^2/\text{d.o.f.} = 485.5/476$ ), giving a plasma temperature of  $25^{(+23)}_{(-5)}$  keV. The 2–10 keV luminosity of the thermal component is  $1.2 \times 10^{41}$  erg/s. The emission measure,  $\sim \int n_{\text{H}}^2 dV$ , is about  $7 \times 10^{63}$  cm $^{-3}$ . Assuming, for self-consistency, that the emitting matter is not optically thick to Thomson scattering, i.e.  $n_{\text{H}} R \sigma_{\text{T}} < 1$  (with  $R$  the radius of the emitting region, assumed spherical and with constant density), then a lower limit to  $R$  of  $7.4 \times 10^{14}$  cm (i.e. about 12 Schwarzschild radii if a value of the black hole mass of  $2 \times 10^8$  solar masses is adopted, Dong & DeRobertis 2006), is obtained (corresponding to an upper limit to  $n_{\text{H}}$  of  $2 \times 10^9$  cm $^{-3}$ ). (If the MEKAL component is used instead of both the hard power law and the highly ionized iron line the fit is still good, the soft power law gets flatter,  $\Gamma = 2.18^{(+0.13)}_{(-0.21)}$  and the thermal plasma 2–10 keV luminosity is  $2.2 \times 10^{41}$  erg s $^{-1}$ .)

The origin and nature of this putative thermal plasma is however unclear. The accretion rate of NGC 3147 is low ( $L/L_{\text{Edd}} \sim 10^{-4}$ , Bianchi et al. 2008), and therefore accretion could occur in a radiatively inefficient mode (ADAF, Narayan et al. 1995; RIAF, Yuan et al. 2003), where the X-ray emission is expected to be due to bremsstrahlung radiation. However, in such a mode the ion temperature is expected to be extremely high, and no visible line is expected. The thermal emission may be related to hot gas in a starburst region, but the implied luminosities are quite large, and there is no evidence for such an extreme starburst at other wavelengths. Alternatively, the plasma emitting region may be a compact one, in the innermost regions of the AGN. While there is so far no strong evidence of a significant contribution of such a plasma emission to the X-ray spectrum of Seyfert galaxies, it must be recalled that NGC 3147 is likely a peculiar source.

### 3.3. The hard X-ray emission

One of the goals of the *Suzaku* observation of NGC 3147 is to exploit its hard X-ray coverage to test the Compton-thick hypothesis for the unabsorbed X-ray spectrum of this Seyfert 2 galaxy. In fact, if the source is Compton-thick, the spectrum may appear unabsorbed because the primary emission below 10 keV would be completely hidden by the thick absorber, the observed emission being due to reflection from circumnuclear matter. In this scenario, the primary emission could emerge above 10 keV (if the absorber is not too thick, see e.g. Matt et al. 1999) and then be observable with the HXD/PIN. As discussed in the previous section, the observed  $EW$ s of the iron lines are consistent with the Compton-thick hypothesis (although in a quite unusual configuration), even if other scenarios are also possible.

In Fig. 6 (left panel), the PIN spectrum is added to the already analyzed XIS spectra, and a clear excess with respect to the extrapolation of the XIS-only best fit model is apparent (the result is basically the same if a high temperature thermal plasma is used to account for the hydrogen-like iron line). No confusing source is known in the PIN field of view, according to the existing catalogs of bright X-ray sources. Assuming that the excess is due to the nuclear radiation piercing through a Compton-thick absorber, we included in the model the transmission and scattering components expected in such a case (Matt et al. 1999). In practice, we added to the model described in the previous section (which in this case should represent the nuclear emission reflected mostly by highly ionized matter) the transmitted and scattered (by the torus) emission using the MYTorus model

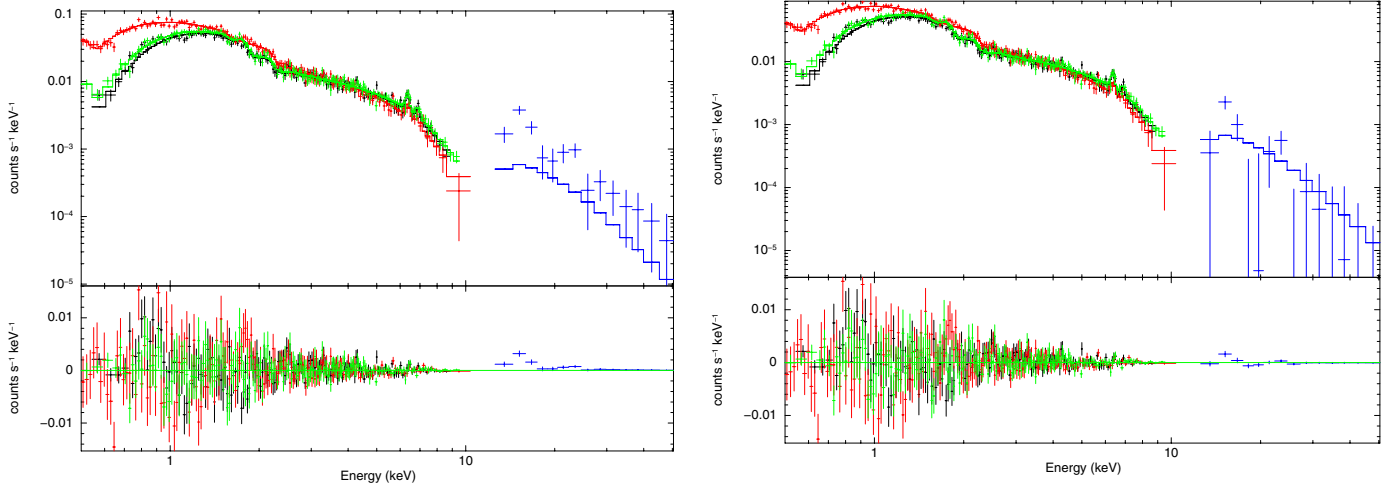


**Fig. 6.** XIS and HXD/PIN spectra fitted with the best fit XIS-only model. A clear excess at hard X-ray is observed (*left panel*), which however disappears (*right panel*) once a 3.5% systematic increase in the background is included (see text for discussion).

(Murphy & Yaqoob 2009; see also <http://www.mytorus.com/>). The inclination angle of the system was fixed to 90 degrees for simplicity. The values of the absorber column density and of the normalization (at 1 keV) of the intrinsic radiation are strongly correlated, and shown in Fig. 7. The normalization of the unabsorbed (reflected in this scenario) power law is about  $4 \times 10^{-4}$  in the same units, which implies that at the 90% confidence level the ratio between primary and reflected components ranges from about 10 to 30, a value somewhat lower than usually found (e.g. Panessa et al. 2006; Marinucci et al. 2012). The 15–100 keV flux of the source is  $1.2 \times 10^{-11}$  erg cm $^{-2}$  s $^{-1}$ . The 2–10/20–100 keV ratio is therefore more typical of Compton-thin sources, according to the diagnostic diagram of Malizia et al. (2007).

This result is only marginally consistent with the upper limit of  $1.3 \times 10^{-11}$  erg cm $^{-2}$  s $^{-1}$  to the 20–100 keV flux obtained by *BeppoSAX* (Dadina 2007) and with the upper limit of  $7 \times 10^{-12}$  erg cm $^{-2}$  s $^{-1}$  to the 20–40 keV flux obtained by *INTEGRAL* on September/October 2009 (this work). It is inconsistent with the *Swift*-BAT observation of this source, which provides only an upper limit to the 15–150 keV flux of  $4 \times 10^{-12}$  erg cm $^{-2}$  s $^{-1}$  (La Parola, priv. comm.). It must be recalled that the PIN spectrum is obtained adopting the standard model for the background, which has an estimated average reproducibility of 3% at  $1\sigma$  (Fukazawa et al. 2009)<sup>3</sup>. For individual observations, however, deviations of the background as high as 5% are sometimes observed (Pottschmidt, priv. comm.). A background higher by 3.5% suffices to reduce the 15–100 keV flux to a value consistent with the *Swift*-BAT upper limit, and in this case no excess is apparent (Fig. 6, right panel). Unfortunately, this observation does not include a period of Earth occultation, so the real level of the background cannot be determined.

#### 4. Conclusions

Based on a short XMM-Newton observation, there were good arguments against the Compton-thick hypothesis for NGC 3147 (Bianchi et al. 2008): the X-ray/[OIII] ratio is typical of

<sup>3</sup> The cosmic X-ray background is also highly variable, up to 10%, from place to place on scales of 1 sq degree (Barcons et al. 2000). However, the CXB is only 5% of the total PIN background (Fukazawa et al. 2009).

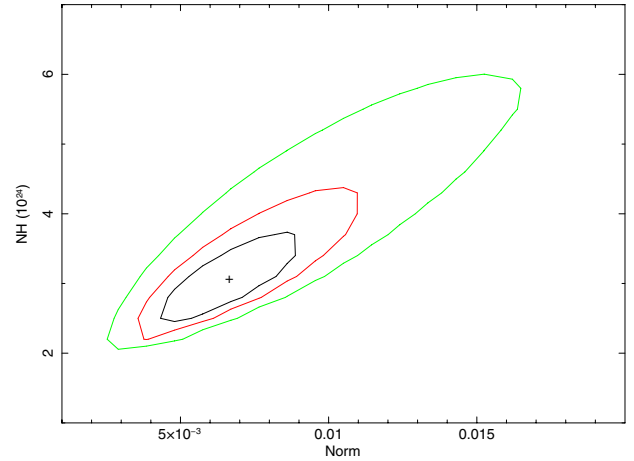


**Fig. 7.** Contour plot of the putative Compton-thick absorber column density vs. normalization of the primary power-law.

unobscured objects, as well as the X-ray spectrum: in Compton-thick sources the 2–10 keV emission is usually much harder, being dominated by the Compton reflection component from low ionization matter and with a neutral iron line of about 1 keV EW.

However, if reflection is from highly ionized matter the spectrum is steeper, but in this case emission from He- or H-like ions is also expected (Matt et al. 1996). Our *Suzaku* observation suggests the presence of a strong H-like line. Indeed, the overall line and continuum spectrum below 10 keV is consistent with a Compton-thick scenario in which reflection is mostly (but not entirely) due to a highly ionized mirror. Interestingly, if this is the case, the absorber may not be the torus, which in this source is claimed by Shi et al. (2010) to be seen almost face-on. Strong highly ionized reflectors in Compton-thick Seyfert 2s are rare, and even when observed, as in NGC 1068, their relative importance with respect to the low ionization reflector is lower (Iwasawa et al. 1997; Matt et al. 2004). NGC 3147 would therefore be rather extreme. It is worth noting that a larger-than-usual amount of highly ionized reflection may at least partly explain the unusually (for a Compton-thick source) high X-ray/[OIII] ratio, as well as the low primary-to-reflection ratio.

On the other hand, it must also be stressed that alternative hypotheses, like e.g. large iron overabundance or a line emission

from a very hot (temperature of about 20 keV), optically thin plasma cannot be ruled out. These characteristics would be unusual in Seyfert galaxies, but NGC 3147, if confirmed as a “true” Seyfert 2 galaxy, would be a peculiar source anyway.

A strong argument against the Compton-thick scenario is provided by the observed flux variation between the *Suzaku* and the *XMM-Newton* observations, obtained 3.5 years apart. Flux variations on yearly time scales were also found comparing earlier observations with *ASCA*, *BeppoSAX* and *Chandra*. These variations indicate that we are looking at an emitting region with a size smaller than a parsec. On the other hand, the argument, albeit strong, is still not decisive. Variations on similar or even smaller time scales have been claimed for NGC 1068, the archetypal Compton-thick Seyfert 2 (Guainazzi et al. 2000; Colbert et al. 2002). Interestingly, in NGC 1068 the variations seems to concern the highly ionized reflector, which in that source is prominent only above about 2 keV (reflection from less ionized matter, possibly related to the Narrow Line Regions, dominates at lower energies). Moreover, there is evidence in some sources, most notably NGC 1365 (Risaliti et al. 2005), of Compton-thick material very close to the central black hole.

If the source is moderately Compton-thick, we expect that the direct emission would pierce through the absorber in hard X-rays. Using the standard background subtraction, an excess in the PIN is observed, which however disappears – becoming consistent with the *Swift*/BAT upper limit – assuming that the background is higher than usual by 3.5%, a not uncommon variation. Therefore, this observation is unfortunately not decisive in this respect.

To conclude, after the new *Suzaku* observation the “true” Seyfert 2 nature of NGC 3147 remains the most probable hypothesis. On the other hand, the ionized iron line is best explained in the “highly ionized reflector” Compton-thick scenario, which is still a viable option. Future sensitive hard X-ray observations with *NuStar* and/or high spectral resolution observations with *Astro-H* are needed to definitely settle the issue.

*Acknowledgements.* We thank the anonymous referee for her/his valuable suggestions. Katja Pottschmidt is gratefully acknowledged for her help on the

PIN background, and Valentina La Parola for providing the *Swift*/BAT upper limit to the flux of the source. G.M., S.B. and F.P. acknowledge financial support from ASI under grants ASI/INAF I/088/06/0 and I/009/10/0, F.P. also from grant INTEGRAL I/033/10/0. X.B.’s research is funded by the Spanish Ministry of Economy and Competitiveness through grant AYA2010-21490-C02-01.

## References

- Anders, E., & Grevesse, N. 1989, *Geo. Cosm. Acta*, 53, 197  
 Antonucci, R. R. J. 1993, *ARA&A*, 31, 473  
 Balucinska-Church, M., & McCammon, D. 1992, *ApJ*, 400, 699  
 Barcons, X., Mateos, S., & Ceballos, M. T. 2000, *MNRAS*, 316, L13  
 Bianchi, S., & Matt, G. 2002, *A&A*, 387, 76  
 Bianchi, S., Corral, A., Panessa, F., et al. 2008, *MNRAS*, 385, 195  
 Colbert, E. J. M., Weaver, K. A., Krolik, J. H., et al. 2002, *ApJ*, 581, 182  
 Dadina, M. 2007, *A&A*, 461, 1209  
 Dickey, J. M., & Lockman, F. J. 1990, *ARA&A*, 28, 215  
 Dong, X. Y., & De Robertis, M. M. 2006, *AJ*, 131, 1236  
 Elitzur, M., & Shlosman, I. 2006, *ApJ*, 648, L101  
 Fukazawa Y., Mizuno, T., Watanabe, S., et al. 2009, *PASJ*, 61, 17  
 Iwasawa, K., Fabian, A. C., & Matt, G. 1997, *MNRAS*, 289, 443  
 Garcia, J., Kallman, T. R., & Mushotzky, R. F. 2011, *ApJ*, 731, 131  
 Guainazzi, M., Molendi, S., Vignati, P., Matt, G., & Iwasawa, K. 2000, *New Astron.*, 5, 235  
 Malizia, A., Landi, R., Bassani, L., et al. 2007, *ApJ*, 668, 81  
 Marinucci, A., Bianchi, S., Nicastro, F., & Matt, G. 2012, *ApJ*, submitted  
 Matt, G., Fabian, A. C., & Ross, R. R. 1993, *MNRAS*, 262, 179  
 Matt, G., Fabian, A. C., & Ross, R. R. 1996a, *MNRAS*, 278, 1111  
 Matt, G., Brandt, W. N., & Fabian, A. C. 1996b, *MNRAS*, 280, 823  
 Matt, G., Fabian, A. C., & Reynolds, C. S. 1997, *MNRAS*, 289, 175  
 Matt, G., Pompilio, F., & La Franca, F. 1999, *New Astron.*, 4/3, 191  
 Matt, G., Bianchi, S., Guainazzi, M., & Molendi, S. 2004, *A&A*, 414, 155  
 Nicastro, F. 2000, *ApJ*, 530, L65  
 Nicastro, F., Martocchia, A., & Matt, G. 2003, *ApJ*, 589, L13  
 Murphy, M. K. D., & Yaqoob, T. 2009, *MNRAS*, 397, 1549  
 Narayan, R., Yi I., & Mahadevan, R. 1995, *Nature*, 374, 623  
 Panessa, F., Bassani, L., Cappi, M., et al. 2006, *A&A*, 455, 173  
 Ptak, A., Yaqoob, T., Serlemitsos, P. J., Kunieda, H., & Terashima, Y. 1996, *ApJ*, 459, 542  
 Risaliti, G., Elvis, M., Fabbiano, G., Baldi, A., & Zezas, A. 2005, *ApJ*, 623, L93  
 Ross, R. R., & Fabian, A. C. 1993, *MNRAS*, 261, 74  
 Shi, Y., Rieke, G. H., Smith, P., et al. 2010, *ApJ*, 714, 115  
 Terashima, Y., & Wilson, A. S. 2003, *ApJ*, 583, 145  
 Tran, H. D., Lyke, J. E., & Mader, J. A. 2011, *ApJ*, 726, L21  
 Yuan, F., Quataert, E., & Narayan, R. 2003, *ApJ*, 598, 301